

Kinetics of the Precipitation of Human Fibrinogen by ZnCl_2 and CuCl_2

Takaaki KISHI, Hiroshi MAEDA,* and Shoichi IKEDA

Department of Chemistry, Faculty of Science, Nagoya University, Chikusa-ku, Nagoya 464

(Received December 8, 1982)

Kinetics of the precipitation of human fibrinogen by the addition of ZnCl_2 was followed by the turbidity at 350 or 500 nm. Fast or slow precipitation occurred depending on whether the metal concentration (C_M) was higher or lower than its critical value. In fast precipitations, the turbidity reached the stationary value within about 30 min. From the stationary values of the turbidity the critical concentration could be determined. A sigmoidal increase of the turbidity was often observed at low protein concentrations (C_P); the lag time decreased with both C_M and C_P . At the final stage of the precipitation, the turbidity reached the stationary value exponentially; the characteristic time constant was almost independent of both C_M and C_P . These kinetic behaviors were consistent with the gelation model proposed to the present precipitation. When CuCl_2 was used in place of ZnCl_2 , similar kinetic behaviors were obtained in many respects, suggesting the similar mechanism of precipitation for both ZnCl_2 and CuCl_2 . Changes from slow to fast precipitation were observed when ionic strength was lowered.

In the preceding paper,¹⁾ the precipitation of human fibrinogen was examined and the process was shown to be best understood as a kind of gelation where the extent of reaction did not exceed a limit even when gelation was completed. Also an interesting result was obtained in the study that the turbidity was linearly related to the 'solubility' of the protein.¹⁾ Here and throughout the present study, the term solubility does not refer to a thermodynamic phase equilibrium but only represents the protein concentration in the supernatant. The time course of the turbidity can be interpreted as the time course of the solubility in the precipitation of human fibrinogen by ZnCl_2 . This situation is different from that frequently encountered in the kinetics of coagulation of colloids, where the turbidity is a complex quantity and only its initial changes are used to extract information on the coagulation. In the present study, kinetics of precipitation of human fibrinogen was followed by the turbidity at different protein concentrations and at various ZnCl_2 or CuCl_2 concentrations.

The interaction of fibrinogen with CuCl_2 could not be studied in the previous study,¹⁾ because the measurement of the solubility was hampered by the interaction of CuCl_2 with Tris buffer.²⁾ Since the absorbance at 350 or 500 nm is little affected by the interaction of CuCl_2 with Tris buffer, the effect of CuCl_2 on the precipitation of human fibrinogen can be studied in the present study by following the time course of the turbidity.

Experimental

Fibrinogen, ZnCl_2 , CuCl_2 , and Tris were the same as used in the previous studies.^{1,2)}

In the kinetics of precipitation, the mixing of ZnCl_2 (or CuCl_2) solutions was carried out by pushing down a plunger until it reached the bottom of a cell followed by pulling it up. The cell was placed in the light path of a spectrophotometer. In this way, 0.01 to 0.1 cm^3 of metal chloride solution in a basket attached to the end of a plunger could be mixed with a protein solution (3–4 cm^3) contained in a cell. The change of the absorbance (turbidity) was automatically recorded on a recorder (chart speed 0.2 cm/s). It took less than one second for this single down and up manual motion. The extent of uniform mixing was checked using a dye solution. It was found that about 99% of the

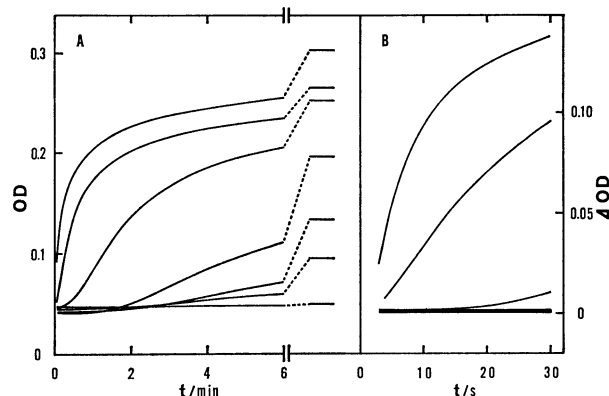


Fig. 1. Time courses of the turbidity at 350 nm at the protein concentration of 0.078 g dm^{-3} .

ZnCl_2 concentrations (mol dm^{-3}) (from top to bottom): 3.75×10^{-4} , 1.88×10^{-4} , 9.68×10^{-5} , 7.79×10^{-5} , 6.84×10^{-5} , 4.92×10^{-5} , and 2.97×10^{-5} . In (B), ΔOD represents a change from the original level ($t=0$) at each ZnCl_2 concentration. Stationary values obtained at 25–30 min are indicated with horizontal bars in (A).

final absorbance was obtained by a single down-up motion. It took less than 2 s for two successive motions, which gave a practically complete mixing. Absorption spectra and the turbidity were both measured with a Shimadzu UV-200 S spectrophotometer using a cell of 1 cm light path.

The protein concentration (g dm^{-3}) was determined as described in the preceding paper.¹⁾ ZnCl_2 or CuCl_2 concentration was denoted as C_M and expressed in M (mol dm^{-3}).

Results

I. ZnCl_2 . *Time Course of the Turbidity:* The time course of the turbidity was followed at two protein concentrations, 0.078 and 0.93–0.94 g dm^{-3} . The data obtained at an intermediate concentration (0.23 g dm^{-3}) were given in the preceding paper.¹⁾

Characteristic time courses were most evident at the lowest protein concentration (0.078 g dm^{-3}) as shown in Figs. 1 (A) and (B). At a ZnCl_2 concentration (C_M) of 3.0×10^{-5} M, the turbidity increased slightly and linearly with time. At $C_M = 4.9 \times 10^{-5}$ M, how-

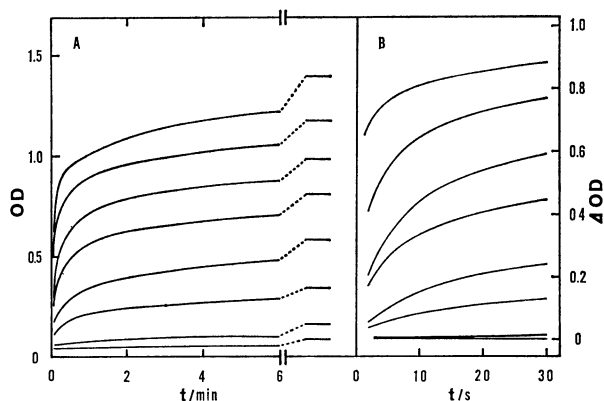


Fig. 2. Time courses of the turbidity at 500 nm at the protein concentration of $0.93\text{--}0.94\text{ g dm}^{-3}$. ZnCl_2 concentrations (mol dm^{-3}) (from top to bottom): 1.88×10^{-4} , 9.68×10^{-5} , 7.79×10^{-5} , 6.84×10^{-5} , 5.88×10^{-5} , 4.92×10^{-5} , 2.97×10^{-5} and 1.99×10^{-5} . In (B), ΔOD represents a change from the original level ($t=0$) at each ZnCl_2 concentration. Stationary values obtained at 25–30 min are indicated with horizontal bars in (A).

ever, a sigmoidal shape began to appear; after a lag time the turbidity began to increase and reached a stationary value after 25–30 min.

Typical sigmoidal patterns were clearly observed for a range of $(6.8\text{--}9.7) \times 10^{-5}\text{ M}$. At ZnCl_2 concentrations larger than $1.9 \times 10^{-4}\text{ M}$, a sigmoidal shape could not be recognized any more in Fig. 1(A). However, when initial stages were closely examined, as shown in Fig. 1(B), then the presence of a lag time was noticed up to $3.8 \times 10^{-4}\text{ M}$, since initial slopes at these concentrations (1.88 to $3.75 \times 10^{-4}\text{ M}$) could not be extrapolated to zero time. Accordingly, the time course can be characterized by a sigmoidal increase when C_M is larger than about $5 \times 10^{-5}\text{ M}$. In this concentration range, the lag time became shorter and the turbidity in the second phase became larger as C_M increased.

At the intermediate protein concentration (0.23 g dm^{-3}), essentially the same kinetic behavior was observed, which was already reported in the preceding paper.¹⁾

At the largest protein concentration ($0.93\text{--}0.94\text{ g dm}^{-3}$), the turbidity at 500 nm was followed. Sigmoidal changes were not observed except at $C_M = 2.97 \times 10^{-5}\text{ M}$, as shown in Figs. 2(A) and (B). However, we assume that the kinetics follow the sigmoidal pattern and that the lag time is only too short to be detected in the time scale of the present experiment. It is to be noted in Fig. 2(A) that the turbidity increases only slightly but rather linearly with time at $C_M = 1.99 \times 10^{-5}\text{ M}$. A slow phase was thus present even at this high protein concentration. This clearly indicates that the slow phase is not identical to the first step of the sigmoidal pattern but it is a different process other than the fast phase.

The Critical ZnCl_2 Concentration C_M^* : As shown in Figs. 1 and 2 and as suggested in the preceding paper, a critical ZnCl_2 concentration C_M^* can be defined from kinetics, above which the turbidity increases rapidly

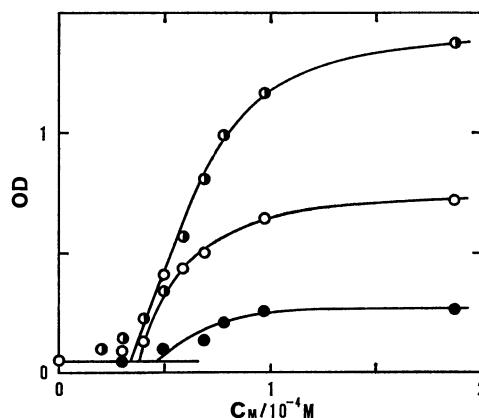


Fig. 3. Stationary turbidities as functions of ZnCl_2 concentration C_M . Protein concentrations (g dm^{-3}): $0.93\text{--}0.94$ (\bullet), $0.22\text{--}0.23$ (\circ), and 0.078 (\bullet). Wavelength: 350 nm (\circ, \bullet) and 500 nm (\bullet).

but in a sigmoidal shape and reaches a stationary value. To evaluate the critical concentration more accurately, the stationary values of the turbidity are plotted against C_M for three protein concentrations in Fig. 3. The data at the intermediate concentration were taken from the preceding paper.¹⁾ When the stationary turbidities obtained from the fast phase are extrapolated to the original level (protein solution in the absence of ZnCl_2), the value of abscissa corresponds to C_M^* . The values are $(4\text{--}5) \times 10^{-5}\text{ M}$ ($(3\text{--}5) \times 10^{-5}\text{ M}$), $(3.5\text{--}4.0) \times 10^{-5}\text{ M}$ ($(3\text{--}4) \times 10^{-5}\text{ M}$), and $(2.5\text{--}3.5) \times 10^{-5}\text{ M}$ ($(2\text{--}3) \times 10^{-5}\text{ M}$), for the protein concentrations of 0.078 , 0.23 and $0.92\text{--}0.94\text{ g dm}^{-3}$, respectively. The values in parentheses are those estimated from a change of the kinetic patterns (from a slow to a fast pattern).

In a previous study, critical concentrations were determined by turbidimetric titrations.²⁾ At a protein concentration of about 1.1 g dm^{-3} , C_M^* was reported as about $4 \times 10^{-5}\text{ M}$ for ZnCl_2 at pH 7.4,²⁾ which approximately coincides with C_M^* determined in the present study for the concentration of 0.94 g dm^{-3} . Accordingly, it is shown that the critical concentrations were adequately assessed in the previous study.²⁾

Lag Times for the Turbidity: In Fig. 4, lag times obtained at different protein concentrations are shown in a logarithmic scale against ZnCl_2 concentration C_M . The kinetic data exhibiting no sigmoidal pattern were interpreted as having lag times smaller than 1 s, and represented on a horizontal line below 1 s in Fig. 4.

At the protein concentration of 0.078 g dm^{-3} , lag times could be determined directly from the kinetic patterns if $C_M < 1 \times 10^{-4}\text{ M}$. For $C_M > 1 \times 10^{-4}\text{ M}$, the lag times were determined as follows. The kinetic data given in Fig. 1(A) were plotted according to the first-order kinetics. A good linearity resulted between $\log(\text{amplitude})$ and the time not only at a later stage of the reaction, which will be discussed in a later section, but also at some initial stage. Here the amplitude of the reaction is defined as $[\text{OD}(\infty) - \text{OD}(t)]$. However, when the linear relation at the

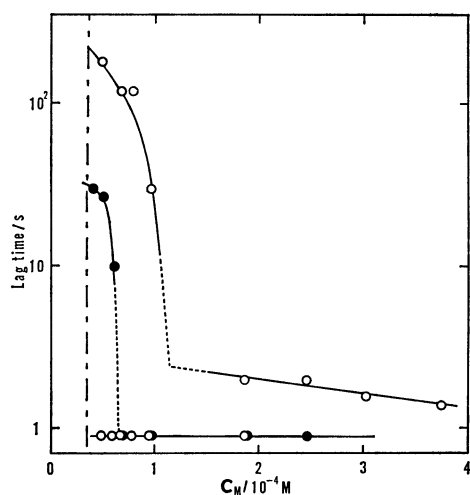


Fig. 4. Dependence of the lag time for the turbidity on ZnCl_2 concentration C_M .

Protein concentrations (g dm^{-3}): 0.93–0.94 (○, on the lowest horizontal line), 0.22–0.23 (●), 0.078 (○). The points on the lowest horizontal line only represent that lag times are less than 1 second. A vertical chain line indicates the approximate location of the critical ZnCl_2 concentration C_M^* (for details see text).

initial stage was extrapolated up to the total amplitude $[\text{OD}(\infty) - \text{OD}(0)]$, the time at the intersection was larger than zero and it was taken as the lag time.

The lag time decreases with an increasing C_M at a given protein concentration; fairly sharply at low ZnCl_2 concentrations and afterwards it becomes almost independent on C_M . The 'transition range' of C_M undoubtedly decreases as the protein concentration decreases. At a protein concentration of 0.93–0.94 g dm^{-3} , the range is probably lower than the critical concentration C_M^* ; the precipitation switches from the slow to the fast phase when C_M exceeds C_M^* , nevertheless lag times are not observed since they are too short to be measured. The dependence of lag times on C_M will be discussed later, where another interpretation of the dependence will be presented. According to the interpretation, the lag times decrease with C_M rather continuously instead of changing in a sharp 'transition' manner.

Initial Rates of the Precipitation: Generally, initial rates of the coagulation of colloids are plotted against the coagulant concentration in a double logarithmic way to find a critical concentration, at which a slow coagulation changes into a fast one. The same procedure is applied to the present kinetic data. When sigmoidal patterns appeared, initial rates were obtained from the slope of the second step.³⁾ For the concentrations lower than C_M^* , initial rates were evaluated as $[\text{OD}(t) - \text{OD}(0)]/t$, where t was taken as 20–30 min.

In Fig. 5, these initial rates are plotted against C_M for three protein concentrations in a double logarithmic way. Unexpectedly, similar results are seen as found in the coagulation of colloids. At each protein concentration, the logarithm of the initial rate linearly increases with $\log C_M$ and then reaches a constant lev-

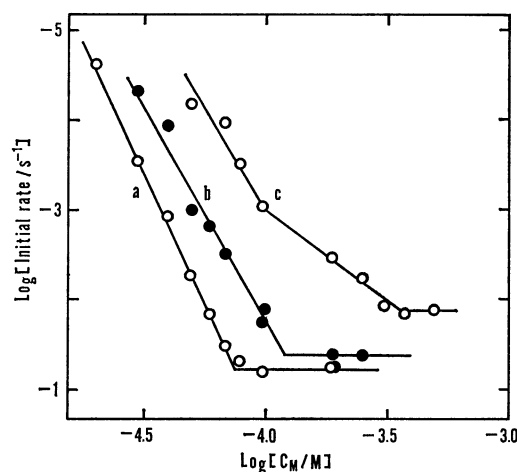


Fig. 5. $\log [d\text{OD}/dt]_{t=0}$ against $\log C_M$ for the precipitation of fibrinogen with ZnCl_2 .

Protein concentrations (g dm^{-3}): (a) 0.93–0.94, (b) 0.22–0.23, (c) 0.078. Optical density: 350 nm (b and c) and 500 nm (a).

el, thus defining a break. It may be argued that the concentration at the break would represent a critical concentration between a slow and a fast coagulation. However, the critical concentration in this sense is given by C_M^* in the present case. It is to be noted that there is no break around C_M^* in Fig. 5. At the lowest protein concentration (curve c), another break occurs around $\log C_M \approx -4$. At the concentration lower than this point, typical patterns were observed as shown in Figs. 1(A) and (B).

It is not fully understood, at present, why the initial rates of the present precipitation formally resemble those of the coagulation of colloids. This point will be discussed later.

Final Stage of the Precipitation: It is stressed in the introduction part that the kinetics of the present precipitation is closely related to that of the solubility. Therefore, the whole time course of the turbidity can, potentially, provide useful information of the present precipitation. However, it is too complicated to be analyzed properly, at present. In the preceding two sections, the initial stage of the kinetics is examined; the lag times and the initial rates.

It was found that the final stage of the present kinetics, shown in Figs. 1 and 2, could be described in terms of a single exponential function of time. Therefore, the amplitude $A(t)$, which is equal to $[\text{OD}(\infty) - \text{OD}(t)]$, can be expressed as Eq. 1.

$$A(t) = A_0(t) + A_1 \exp(-t/\tau) \quad (1)$$

The contribution from the term $A_0(t)$ generally becomes negligible about 3–4 and 6–8 min after the addition of ZnCl_2 , at low and high ZnCl_2 concentrations. Consequently, a fraction larger than 3/4 of the entire time region can be described in terms of a single exponential at all C_M (if $C_M > C_M^*$) and protein concentrations examined. The relative contribution from the exponential term, A_1/A_t , is shown in Fig. 6(A) as functions of C_M at three protein concentrations. The total amplitude A_t is defined as $A_0(0) + A_1$.

At a low protein concentration of 0.08 g dm^{-3} , the

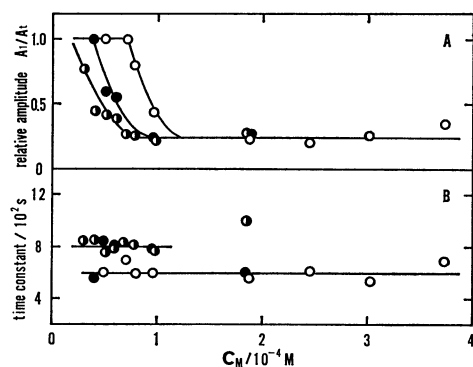


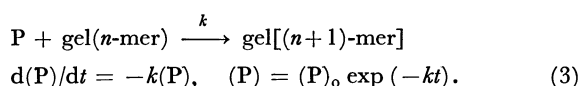
Fig. 6. Relative kinetic amplitude (A_1/A_i) (A) and the characteristic time constant (B) of the final stage of the precipitation as functions of ZnCl_2 concentration C_M . Protein concentrations (g dm^{-3}): 0.93–0.94 (\bullet), 0.22–0.23 (\bullet), and 0.078 (\circ).

ratio A_1/A_i is unity if $C_M \leq 7 \times 10^{-5}$ M. Under this condition, the entire time course can be represented by Eq. 2 using a lag time t_0 ,

$$A(t) = A_1 \exp(-(t-t_0)/\tau) \quad (t \geq t_0). \quad (2)$$

When C_M becomes larger than 7×10^{-5} M, the relative contribution of the exponential term A_1/A_i becomes smaller than unity and decreases further as C_M increases and reaches as low as 0.2 at large C_M values. In other words, the contribution from other fast processes is dominant for C_M larger than 1×10^{-4} M. As the protein concentration increases, the contribution from the fast processes becomes significant even at lower C_M values as shown in Fig. 6(A).

The time constant τ characterizing the final exponential change is independent of C_M and only slightly dependent on the protein concentration as shown in Fig. 6(B). At the final stage of precipitation, it is likely that the growth of gel occurs as a unimolecular reaction with respect to a monomer protein (P) in solution.



It is quite reasonable, then, that this rate constant k , which is the reciprocal of τ , is independent of both C_M and protein concentration under the present condition of excess Zn^{2+} ions.

II. CuCl_2 . The time courses of the turbidity were also measured in the case of CuCl_2 at three protein concentrations: about 0.045, 0.23–0.26, and 0.94 g dm^{-3} . Two different kinetic patterns, fast and slow, were also found in the case of CuCl_2 depending on whether CuCl_2 concentration (C_M) was larger or smaller than the critical value C_M^* . Generally, kinetic behavior was similar to that found in the case of ZnCl_2 . These results suggest that the essential mechanism for the fast precipitation is also common to both cases, ZnCl_2 and CuCl_2 .

The critical concentrations obtained from the kinetic studies were: $(3\text{--}3.5) \times 10^{-4}$ M ($(3\text{--}3.9) \times 10^{-4}$ M), $(1.8\text{--}2.0) \times 10^{-4}$ M ($(1.3\text{--}1.8) \times 10^{-4}$ M), and $(1\text{--}1.5) \times 10^{-4}$ M ($(1\text{--}2) \times 10^{-4}$ M) for the protein con-

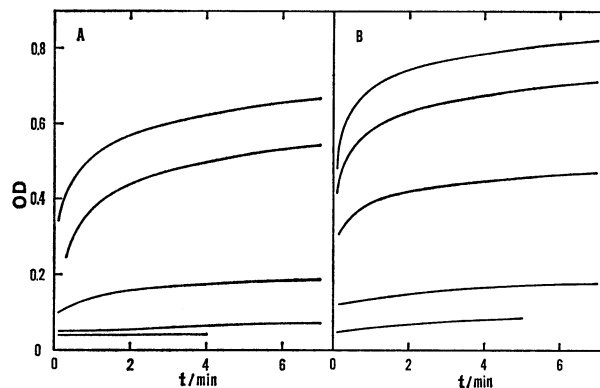


Fig. 7. Effects of ionic strength on the kinetics of precipitation in the case of CuCl_2 . NaCl concentrations (mol dm^{-3}): 0.15 (A) and 0.015 (B). Protein concentrations (g dm^{-3}): 0.23 (A) and 0.26 (B). CuCl_2 concentrations (mol dm^{-3}) (from top to bottom): (A) 3.87×10^{-4} , 3.78×10^{-4} , 2.76×10^{-4} , 1.82×10^{-4} , and 1.25×10^{-4} . (B) 2.86×10^{-4} , 2.35×10^{-4} , 1.82×10^{-4} , 1.25×10^{-4} , 6.45×10^{-5} .

centrations of 0.045, 0.23, and 0.94 g dm^{-3} , respectively. The values in parentheses were estimated from the change of kinetic patterns.

In the case of CuCl_2 , the effect of ionic strength was also examined at the protein concentration of about 0.23–0.26 g dm^{-3} .

The kinetic data obtained at 0.15 and 0.015 M NaCl are presented in Figs. 7 (A) and (B), respectively. At 0.015 M NaCl, a fast pattern was already observed even at $C_M = 6.5 \times 10^{-5}$ M. The critical concentration was thus reduced considerably as ionic strength decreased. This result is consistent with the previous finding²). The critical concentration at 0.015 M NaCl was estimated as about $(0.5\text{--}1.0) \times 10^{-4}$ M from the stationary values of the turbidity.

Discussion

Lag Time for the Turbidity. In the preceding paper, a gelation model was proposed to account for the characteristic features of the present precipitation. The validity of the proposed model is further confirmed in the present kinetic study, since sigmoidal increase of the turbidity is best understood as representing a gelling process. The lag time for the turbidity is no more than the time interval before the extent of reaction reaches the gel point.

According to the classical kinetics of gelation,^{4–6}) the lag time t_0 is given by Eq. 4⁴) for the gelation of N units having f identical functional groups ('homogelation').

$$t_0 = [f(f-2)Nk]^{-1}. \quad (4)$$

Here k denotes the association rate constant, which is not necessarily identical to the rate constant introduced in Eq. 3.

In the present model, gelation among various species has to be considered, such as A_x , $A_{x-1}B$, $A_{x-2}B_2$, and so on. Here x denotes the total number of binding sites per fibrinogen, which was tentatively assumed as three in the preceding paper.¹) The interconversion

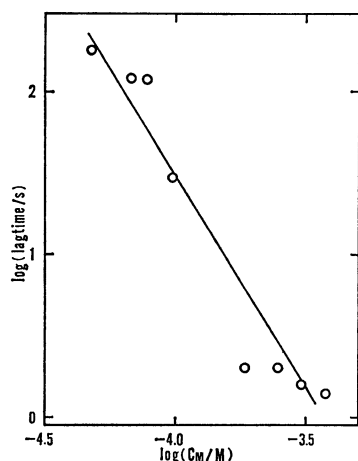


Fig. 8. A double logarithmic plot of the dependence of the lag time on ZnCl_2 concentration C_M . Protein concentration: 0.078 g dm^{-3} .

among these species occurs through the binding equilibria with Zn^{2+} ions. Moreover, the 'bond' is formed only between A and B groups. Therefore, Eq. 4 cannot be applied to the present model in a strict sense. Instead of following the exact kinetic equations relevant to the present model, only a brief discussion is presented here to help understanding the obtained results on the lag time.

The number of units N in Eq. 4 may be approximately equated to the number of various species other than A_x (no zinc ions are bound to it), which is given as

$$N \approx N_p K C_M (1 - K C_M)^{-1}. \quad (5)$$

Here N_p denotes the total number of fibrinogen molecules in solution. If species A_x considerably contributes to the aggregation, then we have to set $N \approx N_p$. Generally, we may write $N \approx N_p (K C_M)^{a'}$, where a' varies between 0 and 1. Since $K C_M$ is much smaller than unity as examined in the preceding paper¹⁾, the number of B groups is much smaller than that of A groups. Consequently, the number of 'functional groups' f in Eq. 4 is roughly proportional to $K C_M x$. Because $K C_M \ll 1$, the term $(f-2)$ in Eq. 4 exhibits a complex dependence on C_M . However, for the moment, we are allowed to write as follows with another parameter a .

$$t_0 \approx N_p^{-1} (K C_M)^{-(2+a)} \quad (0 \leq a \leq 1). \quad (6)$$

At a constant protein concentration, *i. e.*, at a constant N_p , Eq. 6 predicts that $\log(\text{lag time})$ varies linearly

with $\log C_M$ with a slope between -2 and -3 . The data at the lowest protein concentration (0.08 g dm^{-3}) shown in Fig. 4 are replotted in a double logarithmic way in Fig. 8. An approximately linear relation holds with a slope of about -2.6 , consistent with Eq. 6. Unfortunately, the validity of Eq. 6 at higher protein concentrations cannot be examined, since lag times could not be obtained for a wide range of C_M .

Initial Rates of the Precipitation. It is suggested in the preceding paper that the present precipitation is a kind of gelation.¹⁾ Nevertheless, the initial rates of the present precipitation apparently exhibit typical dependence on the 'coagulant' concentration C_M . Although the implication of this unexpected result is not fully understood, the following consideration provides an interpretation of the result.

When Figs. 3 and 5 are compared, it is found that both concentration dependences are very similar. A close relation between the initial rate and the kinetic amplitude (the stationary turbidity) can be shown in the simplest manner, if the turbidity $A(t)$ can be expressed in a single exponential form.

$$A(t) = A_0 \exp(-t/\tau) \quad (7)$$

Then the initial rate $[-(dA/dt)_{t=0}]$ is given as A_0/τ . In this assumed situation, the logarithm of the initial rate is related to $\log A_0$ and $\log \tau$. Accordingly, it can happen that the dependence of the initial rates on C_M is totally ascribed to the dependence of the kinetic amplitude A_0 on C_M . Consequently, if the initial stages of the present precipitation can be described by Eq. 7, with a proper τ , then the results shown in Fig. 5 can be understood as essentially identical to those given in Fig. 3.

We thank Professor M. Tagawa, Nara Women's University, for her kind advice in the construction of the mixing device.

References

- 1) H. Maeda, T. Kishi, and S. Ikeda, *Bull. Chem. Soc. Jpn.*, **56**, 290 (1983).
- 2) H. Maeda, T. Kishi, S. Ikeda, S. Sasaki, and K. Kito, *Int. J. Biol. Macromol.*, in press (1983).
- 3) R. H. Ottewill and A. Watanabe, *Kolloid-Z.*, **170**, 38 (1960).
- 4) W. H. Stockmayer, *J. Chem. Phys.*, **11**, 45 (1943).
- 5) R. M. Ziff, *J. Stat. Phys.*, **23**, 241 (1980).
- 6) R. M. Ziff and G. Stel, *J. Chem. Phys.*, **73**, 3492 (1980).